Shuaishuai Zhu,[1] Dennis Larkin,[1] Shusheng Lu,[2] Candice Inouye,[3] Leena Haataja,[1] Arfah Anjum,[1] Robert Kennedy,[2] David Castle,[3] and Peter Arvan[1]

Monitoring C-Peptide Storage and Secretion in Islet β-Cells In Vitro and In Vivo

Diabetes 2016;65:699–709 | DOI: 10.2337/db15-1264

Human proinsulin with C-peptide–bearing Superfolder Green Fluorescent Protein (CpepSfGFP) has been expressed in transgenic mice, driven by the *Ins1* promoter. The protein, expressed exclusively in β-cells, is processed and stored as CpepSfGFP and human insulin comprising only ~0.04% of total islet proinsulin plus insulin, exerting no metabolic impact. The kinetics of the release of insulin and CpepSfGFP from isolated islets appear identical. Upon a single acute stimulatory challenge in vitro, fractional release of insulin does not detectably deplete islet fluorescence. In vivo, fluorescence imaging of the pancreatic surface allows, for the first time, visual assessment of pancreatic islet insulin content, and we demonstrate that CpepSfGFP visibly declines upon diabetes progression in live lepR$^{db/db}$ mice. In anesthetized mice, after intragastric or intravenous saline delivery, pancreatic CpepSfGFP (insulin) content remains undiminished. Remarkably, however, within 20 min after acute intragastric or intravenous glucose delivery (with blood glucose concentrations reaching >15 mmol/L), a small subset of islets shows rapid dispossession of a major fraction of their stored CpepSfGFP (insulin) content, whereas most islets exhibit no demonstrable loss of CpepSfGFP (insulin). These studies strongly suggest that there are "first responder" islets to an in vivo glycemic challenge, which cannot be replicated by islets in vitro.

While a major thrust of modern diabetes research has concentrated on measuring pancreatic β-cell mass and its loss in pathological states (1), increasing consideration has been given to perturbation of islet function (2,3) as a possible cause of pancreatic exhaustion, especially the loss of β-cell insulin content (4). Certainly, the depletion of islet insulin can be observed in various conditions leading to type 2 diabetes (5); however, to date, imaging of pancreatic insulin content, or insulin secretion, in the pancreata of live animals or humans has not been achievable. With this goal in mind, we initially engineered transgenic mice expressing a fluorescent proinsulin in the hopes of monitoring islet insulin content in vivo (6). Unfortunately, total pancreatic fluorescence in those animals was exceedingly weak, rendering the sensitivity of in vivo fluorescence imaging insufficient unless one or more endogenous *Ins* gene alleles were deleted (6). To overcome this problem, a human proinsulin (hPro)-C-peptide–bearing Superfolder Green Fluorescent Protein (CpepSfGFP) construct (which has 9-amino acid substitutions to enhance GFP protein folding stability and brightness) was designed, and this fluorescent proinsulin was found to faithfully replicate normal trafficking, processing, C-peptide storage, and secretion in pancreatic β-cell lines (7,8).

When considering fluorescent C-peptide as a dynamic reporter of insulin storage and secretion in situ, it is worth noting that overall pancreatic insulin content changes very little as a consequence of acute secretory stimulation (9). On average, the readily releasable insulin pool is thought to comprise ≤2% of the total (10) during the first phase of insulin secretion (11), which lasts <20 min (12). In terms of total pancreatic fluorescence, such a small change should never be detected by imaging. On the other hand, in vivo islets do respond robustly to the absolute concentration (and rate of change) of blood

[1]Division of Metabolism, Endocrinology & Diabetes, University of Michigan Medical Center, Ann Arbor, MI
[2]Department of Chemistry, University of Michigan, Ann Arbor, MI
[3]Department of Cell Biology, University of Virginia, Charlottesville, VA
Corresponding author: Peter Arvan, parvan@umich.edu.

Received 8 September 2015 and accepted 11 November 2015.

This article contains Supplementary Data online at http://diabetes.diabetesjournals.org/lookup/suppl/doi:10.2337/db15-1264/-/DC1.

See accompanying article, p. 542.

glucose (13). Moreover, although rarely cited, it has been reported (14) that, in vivo, acute secretory stimulation in normal animals causes β-cell insulin stores in a subset of islets to become dramatically depleted, which seems incongruent with the general impression that very little pancreatic insulin is released by acute secretory stimulation (9). In the current study, we studied two independent founder lines of *Ins1*-hPro-CpepSfGFP transgenic mice that behave identically and synthesize fluorescent proinsulin exclusively in β-cells. The extent of transgene expression (and the human insulin derived from it) does not affect normal growth or metabolism, but the insulin stored in pancreatic islets can now be visualized and quantified by fluorescence microscopy, even in live animals. This feature allows, for the first time, a morphological estimation of the insulin content of individual islets on the pancreatic surface and dispossession of that insulin content during in vivo insulin secretion in real time.

RESEARCH DESIGN AND METHODS

Materials

Guinea pig anti-insulin, rat insulin-plus-proinsulin radioimmunoassay (RIA) that cross-reacts with other species (RI-13K), and human insulin–specific RIA (HI-14K) were from Millipore; ultrasensitive mouse insulin ELISA (80-INSMSU-E01) was from Alpco; "RIA-grade" BSA was from Sigma-Aldrich.

Transgenic Mice

The hPro-CpepSfGFP construct (i.e., with the Superfolder-GFP cDNA [15] ligated into the *Xho*I site of the human C-peptide coding sequence [7]), driven by the upstream 8.3-kb mouse *Ins1* promoter and downstream 2.5-kb human growth hormone (hGH) minigene that serves as an enhancer (6), was introduced into pronuclei of C57BL/6J fertilized eggs. PCR genotyping of tail-tip genomic DNA from 4-week-old animals used GFP-specific primers (forward primer 5′-AGG TCT ATA TCA CCG CCG ACA-3′ and reverse primer 5′-TGC AGT AGT TCT CCA GCT GGT AG-3′), giving rise to a 400-bp product. Transgenic mice were backcrossed to C57BL/6J. Biochemical and cell biological characterizations in this article used animals derived from two independent mouse lineages originating from founders #207 and #369. Housing and all animal procedures were performed in accordance with the rules and regulations of the Committee on the Use and Care of Animals at the University of Michigan.

To examine GFP expression, tissues were fixed in 10% neutral formaldehyde, dehydrated in a graded ethanol series, and embedded in paraffin; 5-μm-thick sections were cut and deparaffinized in Citrisolv (Fisher), rehydrated followed by antigen retrieval (Retrieve-ALL-1; Covance), and immunostained with chicken anti-GFP 1:1,000 (Abcam) and Alexa Fluor 488–conjugated secondary antibody (Invitrogen). Slides were mounted with Prolong Gold with DAPI (Invitrogen) and imaged using an Olympus FV-500 Confocal Microscope.

Intraperitoneal Glucose Tolerance Testing

Mice were fasted for 16 h, and blood glucose level were measured before intraperitoneal injection of D-glucose (1 mg/g body wt).

Pancreatic Islet Preparation

Ice-cold collagenase (2 mg/2 mL; type V; Sigma-Aldrich) in Hanks' balanced salt solution was injected into the pancreatobiliary duct. The pancreas was excised and further digested for 28 min at 37°C, and islets were separated by Histopaque gradient and handpicked under a dissecting microscope. Islets were cultured overnight in RPMI 1640 medium containing 11.1 mmol/L glucose, 10% FBS, and 1% penicillin-streptomycin (Gibco; Thermo Fisher Scientific). Digital image capture of whole-islet fluorescence used a Nikon Diaphot 200 Microscope (Fig. 1*B*) or an AZ100 Microscope (Fig. 5*D*).

Fluorescence Imaging of Dispersed Primary β-Cells

Isolated islets were dissociated with 0.25% trypsin plus 3 mmol/L EGTA; dispersed β-cells were incubated in RPMI 1640 medium containing 11.1 mmol/L glucose and 10% FBS for 48 h. Before confocal microscopy, cells were fixed in 2% formaldehyde, permeabilized with 0.1% NP-40, incubated in blocking solution, and immunolabeled with mouse anti-GFP and Alexa Fluor 488–conjugated secondary antibody as well as guinea pig anti-insulin and a Cy5-conjugated secondary antibody.

Glucose-Stimulated Insulin Secretion

Islets were preincubated for 1 h at 37°C in Krebs-Ringer bicarbonate HEPES buffer (KRBH) (4.7 mmol/L KCl, 115 mmol/L NaCl, 1.2 mmol/L KH_2PO_4, 1.2 mmol/L $MgSO_4$, 2.56 mmol/L $CaCl_2$, 20 mmol/L $NaHCO_3$, and 16 mmol/L HEPES, pH 7.2) supplemented with 0.2% BSA, followed by 1 h (or 20 min) of incubation in KRBH supplemented with 0.2% BSA in the presence of 2.8 or 25 mmol/L glucose. Media were collected and islets were lysed in boiling SDS-gel sample buffer. Insulin release was measured by a rat insulin-plus-proinsulin RIA that cross-reacts between species, human insulin–specific RIA (Fig. 4), or mouse insulin–specific ELISA (Fig. 5*C*).

Transmission Electron Microscopy

Islets were fixed in 2.5% glutaraldehyde and 2% formaldehyde in 0.1 mmol/L Na cacodylate, pH 7.4 (2.5 h); postfixed in 1% OsO4 in 0.1 mol/L Na cacodylate (2 h); washed in 0.15 mol/L NaCl; stained overnight in 0.5% uranyl acetate, pH 5.5; dehydrated in a graded acetone series; and embedded in EPON; and thin sections were cut and stained with uranyl acetate and lead citrate before examination in a Jeol 1230 Electron Microscope.

SDS-PAGE and Western Blotting

Islet lysates and media were resolved by 4–12% NuPAGE Bis-Tris gels (Invitrogen), electrotransferred to nitrocellulose, and probed overnight at 4°C with primary antibodies against insulin (Linco/Millipore), GFP (Immunology Consultants Laboratories), or α-tubulin (Sigma). Western blots

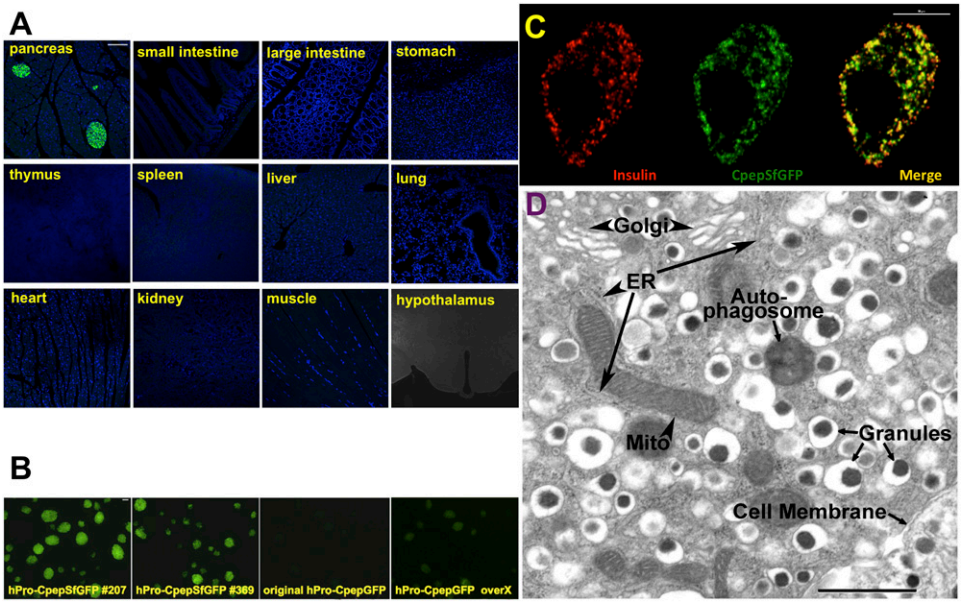

Figure 1—Transgenic expression of hPro-CpepSfGFP. *A*: Sections of various tissues as indicated were examined by indirect immunofluorescence microscopy. As shown, SfGFP expression (green) was detectable only in the endocrine pancreas (n = 6 independent animals examined). DAPI nuclear staining is shown in blue. Scale bar = 100 μm. *B*: Isolated islets from hPro-CpepSfGFP transgenic mice (lines 207 and 369; n = 5 independent animals) and islets from previously reported hPro-CpepGFP transgenic mice (6) were examined for epifluorescence at identical exposure. Scale bar = 100 μm. The panel at far right is an overexposure (overX) of the original hPro-CpepGFP islets. *C*: Dispersed β-cells (n = 6 independent animals) were examined by immunofluorescence for insulin (red) and CpepSfGFP (green); one cell is shown with ×100 objective. Scale bar = 10 μm. *D*: Representative transmission electron micrograph of cytoplasm from a β-cell of hPro-CpepSfGFP transgenic mice. Scale bar = 1 μm. ER, endoplasmic reticulum.

were developed with enhanced chemiluminescence, and quantified using ImageJ Software.

Single-Islet Perifusion

Single islets in heated chambers were perifused (not under pressure) at 0.6 μL/min in etched microchips allowing for continuous small-volume sampling of insulin release (by competitive immunoassay, at 8-s intervals) and quantitative SfGFP fluorescence release from sequential electropherograms, as described (16).

Single β-Cell Real-Time CpepSfGFP Secretion

Dispersed islet β-cells were preincubated for 1 h in standard KRBH (including 5.5 mmol/L glucose, 4.4 mmol/L KCl, and 110 mmol/L NaCl plus 1 mg/mL BSA) on a 37°C heated microscope stage. Once an imaging field was located, the perfusion of cells was initiated with a depolarizing KRBH solution (including 5.5 mmol/L glucose, 60 mmol/L KCl, and 54.4 mmol/L NaCl, plus 1 mg/mL BSA), and image capture included a continuous series of 200-ms exposures (i.e., 5 frames/s).

Live Mouse Pancreatic Imaging

Mice were anesthetized with isoflurane inhalation (plus oxygen at 1 L/min); the surgical site was shaved and cleaned, and mice were placed on a warm sterile stage. Live mouse pancreas fluorescence was performed as previously described (6); additional details are included in the RESULTS section. To measure blood flow to the pancreas, jugular vein injections of uranine (5 mg/mL) were administered followed by live animal fluorescence image capture of the pancreatic surface. All digital fluorescence images of the live mouse pancreas were captured using a Nikon AZ100 Microscope equipped with a Photometrics CoolsnapEZ Digital Camera. In some experiments, immediately after imaging, the incision was closed and the mouse recovered in a warmed padded cage—all mice recovered uneventfully. Reimaging of the mouse pancreas was taken 2 weeks later following the same procedure. Digital images of SfGFP intensity and pancreas area were quantified with MetaMorph Software.

For intragastric or intravenous glucose response, after anesthesia and exposure of pancreas as above, saline (as a negative control) or glucose (4 mg/g body weight intragastric; 1 mg/g intravenous) was administered. Fluorescence images were captured as above at 0, 10, and 20 min after injection. Simultaneously, the tail vein blood glucose concentration was measured by glucometer. The integrated fluorescence intensity of each islet at these time points was analyzed with MetaMorph Software.

Statistical Analysis

Results are presented as the mean ± SEM, calculated using GraphPad Prism Software version 5.0. Statistical differences were determined using a two-tailed Student t test or ANOVA, with a significant value at $P < 0.05$.

RESULTS

Generating hPro-CpepSfGFP Transgenic Mice

We generated founder mice (transgene positive by PCR) expressing hPro-CpepSfGFP, driven by the 8.3-kb mouse *Ins1* promoter, which transmitted the transgene to progeny with expected Mendelian ratios. None of the transgenic lines exhibited a pathological phenotype. The two lines with the strongest transgene expression were derived from founders #207 and #369 (Supplementary Fig. 1), and the results using animals derived from both founders were identical. Five-micron paraffin tissue sections were examined by fluorescence microscopy: we could not detect fluorescent protein expression in the small intestine, large intestine, stomach, thymus, spleen, liver, lung, heart, kidney, muscle, or hypothalamus (Fig. 1*A*). Indeed, fluorescence derived from hPro-CpepSfGFP was detected only in the pancreas, in an islet distribution (Fig. 1*A*). All isolated islets from the progeny of both founders were strongly positive for epifluorescence compared with those of the original hPro-CpepGFP transgenic mice (6), which lack Superfolder-GFP substitutions and can be detected only upon overexposure (Fig. 1*B*). Isolated islets were dissociated into single cells, fixed, permeabilized, and processed for immunofluorescence with anti-insulin. All cells expressing hPro-CpepSfGFP also were labeled positively with anti-insulin in a colocalizing, punctate distribution (Fig. 1*C*). These β-cells exhibited entirely normal cellular ultrastructure, including nondistended endoplasmic reticulum, stacked Golgi cisternae, abundant insulin secretory granules, healthy-appearing mitochondria, and autophagosomes and lysosomes (Fig. 1*D*).

hPro-CpepSfGFP Is Efficiently Processed to Fluorescent C-Peptide

Isolated islets from hPro-CpepSfGFP transgenic mice were examined by reducing SDS-PAGE and Western blotting with anti-GFP. Two main bands were identified at 36 and 32 kDa (Fig. 2*A*). These bands correspond to fluorescent proinsulin (hPro-CpepSfGFP) and fluorescent C-peptide (CpepSfGFP), respectively, and the pattern appeared similar to that from Western blotting with anti-insulin (Fig. 2*B*). By quantitative densitometry, it was apparent that ~85% of the transgene product from both founder lines is processed to the mature fluorescent C-peptide in the steady state (Fig. 2*C*), which is consistent with the abundance of mature granules in the β-cells of these animals (Fig. 1*D*).

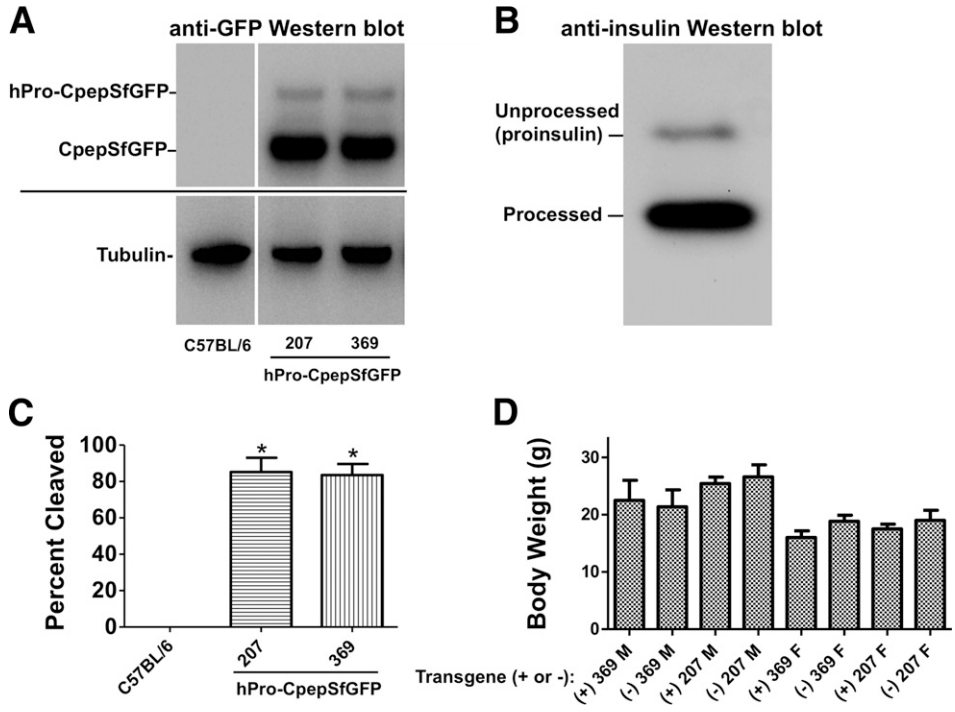

Figure 2—Preliminary characterization of hPro-CpepSfGFP mice. *A*: Isolated islets from hPro-CpepSfGFP mice were lysed and were resolved by SDS-PAGE and Western blotting with anti-GFP. The unprocessed hPro-CpepSfGFP precursor and mature CpepSfGFP from representative animals derived from lines 207 and 369 are shown. Western blotting for α-tubulin is shown as a loading control. *B*: Western blotting of normal mouse islets with anti-insulin to detect unprocessed proinsulin and mature processed insulin. *C*: Quantitative densitometric analysis of anti-GFP immunoblots like those from panel *A*; $n = 7$ animals examined for panels *A* and *B*; $^*P < 0.05$ compared with C57BL/6 mice. *D*: Body weights of 8-week-old transgenic and gender-matched nontransgenic control mice. Values are expressed as the mean ± SEM. $n = 5$–10 per group.

hPro-CpepSfGFP Mice Synthesize Very Limited Quantities of Human Insulin

There were no significant differences in body weight between transgenic and nontransgenic littermates (Fig. 2*D*). Further, both fasting blood glucose and intraperitoneal glucose tolerance were identical in transgenic and nontransgenic animals (Fig. 3*A–D*). Moreover, there were no significant differences between transgenic and nontransgenic littermates in insulin levels in the circulation after either fasting or acute stimulation (30 min) (Fig. 3*E*). Even after 6 months of age, transgenic animals maintained normal glucose tolerance (Fig. 3*F*). In short, we could detect no metabolic effect of hPro-CpepSfGFP expression in transgenic mouse islets. Yet, the bright fluorescence of hPro-CpepSfGFP islets implies a contribution of human insulin to the total insulin plus proinsulin present in these animals. To examine this, islets from control C57BL/6 mice and hPro-CpepSfGFP mice were extracted and total insulin-plus-proinsulin levels were measured using an RIA that cross-reacts between species and does not discriminate between proinsulin and insulin. No significant changes in total insulin-plus-proinsulin level were found in the islets of transgenic mice (Fig. 4*A*). However, by human-specific insulin assay it was apparent that only ~0.04% of total insulin plus proinsulin was composed of human insulin in these islets (Fig. 4*B*). Nevertheless, this was sufficient to detect both unstimulated and stimulated secretion of human insulin from isolated islets (Fig. 4*C*), and this secretion occurred in parallel with the release of endogenous mouse insulin (Fig. 4*D*).

CpepSfGFP Is Stored and Released in Parallel With Endogenous Mouse Insulin

To examine the release of stored secretory granule contents, we stimulated isolated islets in vitro. By Western blotting with anti-GFP, it was clear from static incubations that within 5 min of plasma membrane depolarization, both (mouse) insulin and (human) CpepSfGFP were coreleased into the medium (Fig. 5*A*, left). The same was true when raising extracellular glucose from 2.8 to 25 mmol/L (Fig. 5*A*, right). We also followed secretion from single islets by perifusion, monitoring secretion with a competitive insulin immunoassay within 8 s of release, using a microfluidics device for delivery to the assay chamber (16). In parallel, we followed the release of green fluorescence from single islets in real time. Although it has been suggested that some cosecreted insulin is released from β-cells more slowly than GFP-tagged C-peptide (17), we could not—over multiple individual islets analyzed—discern any significant

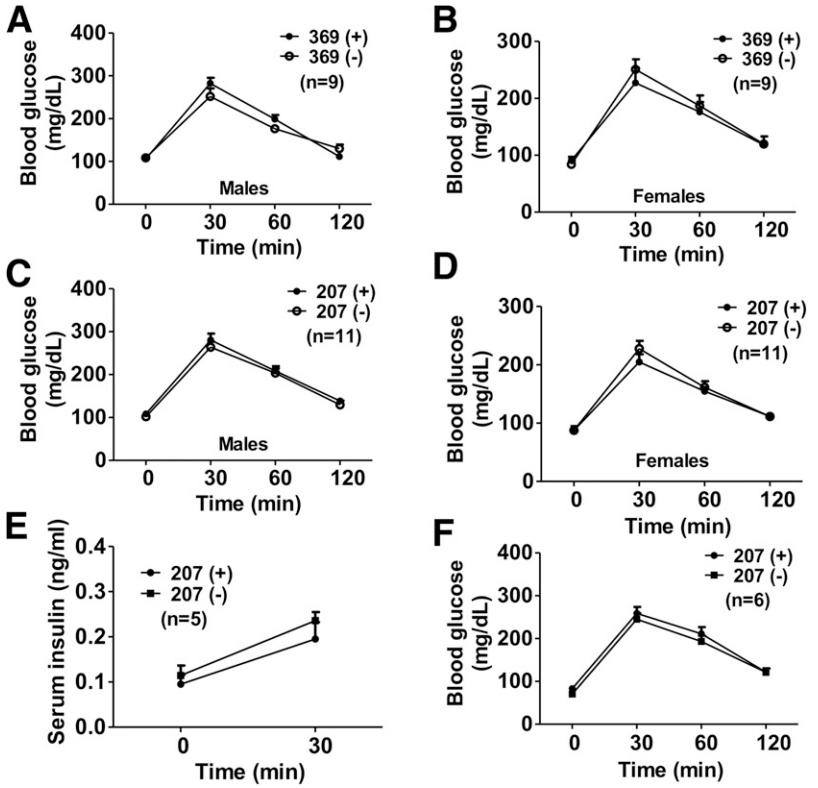

Figure 3—hPro-CpepSfGFP transgenic mice exhibit normal carbohydrate metabolism. Fasting blood glucose and intraperitoneal glucose tolerance test (IPGTT) in hPro-CpepSfGFP transgenic mice and nontransgenic littermates, matched for gender, in lines 369 (*A* and *B*) and 207 (*C* and *D*), with no significant differences. *E*: Circulating insulin levels were screened at 0 min (fasting) and 30 min after initiating the IPGTT, with no significant differences. *F*: IPGTT was repeated in 6.25-month-old transgenic and nontransgenic males, with no significant differences. Values are expressed as the mean ± SEM. *n*, number is shown in the panels.

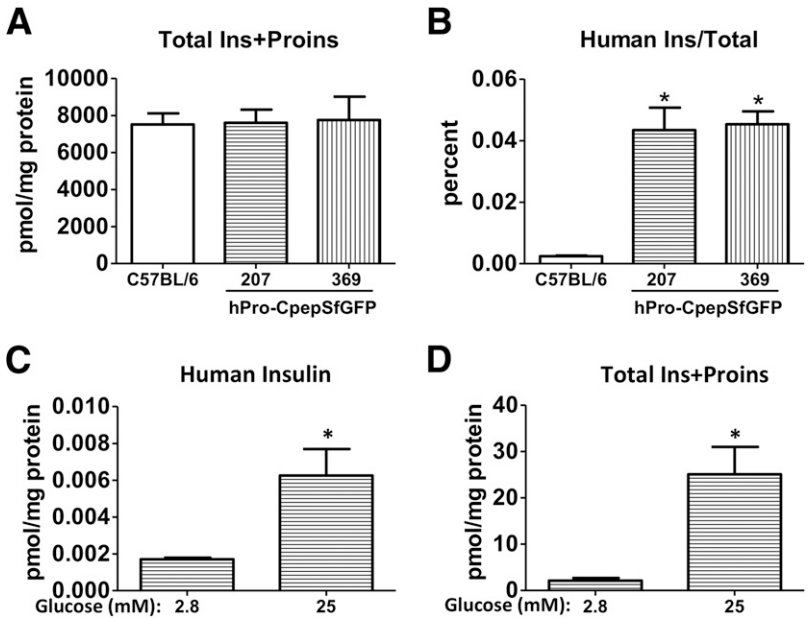

Figure 4—Transgenic hPro-CpepSfGFP mice have normal insulin levels. *A*: Total insulin-plus-proinsulin (Ins+Proins) levels (derived primarily from the endogenous *Ins1* and *Ins2* gene products) in islet lysates of hPro-CpepSfGFP transgenic mice (lines 207 and 369; $n = 5$ independent animals for panels *A* and *B*) and negative control C57BL/6 mice. *B*: In transgenic hPro-CpepSfGFP mice, >99.9% of total Ins+Proins is mouse derived; ~0.04% is human insulin. We do note a small cross-reacting signal in the human-specific insulin assay that can be detected even in mouse-derived samples that contain little or no human insulin. Human insulin secretion (*C*) is stimulated in parallel with mouse insulin secretion (*D*) from isolated islets of hPro-CpepSfGFP mice incubated at 25 mmol/L glucose. $n = 6$ independent animals for panels *C* and *D*. Values are expressed as the mean ± SEM.

kinetic differences between CpepSfGFP and endogenous insulin secretion (Fig. 5*B*). However, when a pooled population of islets was stimulated in the short term to release insulin (Fig. 5*C*) simultaneous with fluorescence microscopy, we could not discern an appreciable decrease in fluorescence in individual islets in vitro (Fig. 5*D*), and overall fluorescence in the islets remained constant (Fig. 5*E*). These findings are consistent with those of reports (9) that only a small fraction (≤2%) of islet insulin content is discharged during acute insulin secretion. To reliably detect insulin secretion by fluorescence in vitro, we stimulated dispersed islet β-cells with either KCl or high glucose and monitored exocytosis by spinning disk confocal microscopy (Supplementary Video 1, beginning ~30 s after secretagogue addition). A frame-by-frame dissection at 200-ms intervals showed multiple flashes (Fig. 6*A*)—the rapid rise of fluorescence that occurs upon granule fusion with plasma membranes followed by a rapid loss of fluorescence as the released content disperses (Fig. 6*B*)—indicating granule exocytosis (18) (Supplementary Video 1). The same characteristics of exocytosis were observed upon depolarization with KCl (Supplementary Video 1 and Fig. 6*B*) and stimulation with high glucose (data not shown), but were undetectable under basal conditions. Altogether, these data clearly establish that CpepSfGFP release from islets is costored and cosecreted with endogenous insulin via discrete exocytotic events (Figs. 5*A* and *B* and 6*A* and *B*), but secretory stimulation in vitro does not appreciably deplete insulin stores from any individual islet (Fig. 5*D* and *E*).

Loss of Pancreatic CpepSfGFP During Progression of Diabetes

Because CpepSfGFP is a parallel marker of endogenously stored insulin, we exploited survival surgery using epifluorescence imaging of the pancreatic surface in vivo to estimate insulin content in the pancreatic tail region (6). Briefly, a small, left-sided, longitudinal incision was used to expose the tail and part of the body of the pancreas (maintaining splenic vascular connections), which was placed on a glass slide and overlayed with a glass coverslip above at a 1.5-mm tissue thickness (using plastic spacers including a fluorescent ruler, between the layers of glass). Blood flow to the pancreas was unimpeded by these manipulations as judged by vascular delivery of uranine to the pancreas within 2 s after tail vein injection (Fig. 6*C*).

Pancreata of live C57BL/Ks lepR$^{db/+}$ and lepR$^{db/db}$ male mice were examined at 5 weeks when animals were normal or prediabetic, respectively, and again at 7 weeks when the lepR$^{db/db}$ males had progressed to diabetes as diagnosed by elevated random blood glucose. The *db*/+ heterozygous males never developed diabetes and never decreased (indeed, tended to increase) their pancreatic surface fluorescence as body growth progressed to completion at 7 weeks (Fig. 7*A*, top panels including blood glucose, and Fig.7*B*, left). By contrast, *db*/*db* homozygous

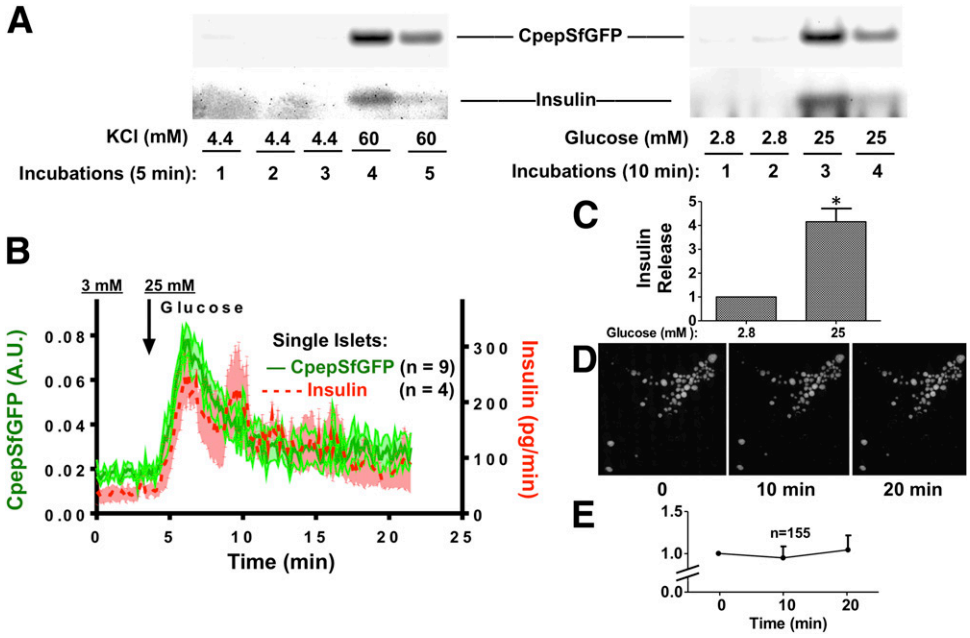

Figure 5—Kinetics of transgenic CpepSfGFP and mouse insulin from isolated hPro-CpepSfGFP islets. *A*: Islets were incubated sequentially in nonstimulating bathing medium (4.4 mmol/L KCl [left] or 2.8 mmol/L glucose [right]) and then in secretagogue-containing bathing medium (60 mmol/L KCl [left] or 25 mmol/L glucose [right]). The media were collected and analyzed by SDS-PAGE and Western blotting with anti-GFP (top panels) or anti-insulin (bottom panels); $n = 5$ independent experiments. *B*: Single islets were microperfused at 3 mmol/L glucose and then switched to 25 mmol/L glucose (arrow at top). Single-islet secretion was measured by the release of GFP fluorescence (averaging of nine single-islet traces is shown by the dark solid line, with the lighter surrounding area showing the SEM on these measurements) and by competitive immunoassay for insulin (averaging of four single-islet traces shown in dashed line, with lighter surrounding area showing the SEM of these measurements), both at 8-s intervals throughout a 22.5-min time course. *C*: Insulin secretion (measured by RIA) from isolated islets in 20-min static incubations of unstimulated (2.8 mmol/L = 50 mg/dL) and then stimulated (25 mmol/L = 450 mg/dL) glucose. Insulin release is plotted as the fold increase upon stimulation; the stimulated secretion corresponds to ~6 pg of immunoreactive insulin per islet. *D*: Simultaneous epifluorescence imaging of isolated islets during the 20 min of stimulation at 25 mmol/L glucose (representative of $n = 5$ independent experiments for panels *C*, *D*, and *E*). *E*: Individual islet fluorescence during experiments like those shown in panel *D* was quantitated, and the percentage change for each islet calculated at each time point. No individual islets exhibited a 50% change in fluorescence in any of these stimulation experiments; the average fractional change in individual islet fluorescence during glucose stimulation is plotted in the figure.

males all developed diabetes, and all showed a significant decline of pancreatic surface fluorescence as they advanced from puberty to adulthood (Fig. 7*A*, bottom panels including blood glucose, and Fig. 7*B*, right). During this same time course, *db*/*db* homozygotes are known to experience a decline in pancreatic insulin content (19); thus, our data strongly suggest that pancreatic surface epifluorescence is a useful indicator to follow changes in pancreatic insulin content of any individual hPro-CpepSfGFP mouse over time.

Dynamic Analysis of In Vivo Pancreatic Insulin (CpepSfGFP) Secretion

To follow pancreatic insulin (CpepSfGFP) secretion in real time during a nutrient challenge, we prepared live anesthetized mice for imaging of the pancreatic surface upon acute administration of glucose (or saline as a negative control) at 0, 10, and 20 min, and individually examined and quantified the fold change in fluorescence intensity from every islet in the field. After intragastric administration of saline (Fig. 8*A*, a representative image shown with time points vertically aligned), some islets modestly increased and others modestly decreased in fluorescence intensity, but no islet from the entire group of negative control animals ever exhibited more than a 50% change in fluorescence intensity during the time course, and, overall, there was no loss of average islet fluorescence (Fig. 8*B*). After intragastric administration of glucose in vivo sufficient to raise blood glucose levels in the short term to ≥280 mg/dL, fluorescence intensity of most islets remained unchanged (Fig. 8*C*), as they did in vitro (Fig. 5*D*). However, in vivo, a small subfraction (≤20%) of islets of stimulated mice showed a major decrease in fluorescence intensity (>50% loss) that can be explained only by degranulation of a major fraction of β-cells of that islet (Fig. 8*C* [quantified in Fig. 8*D*]). This was consistently replicated in multiple animals and was never observed under control conditions. These experiments were then repeated using intravenous glucose administration (Fig. 8*E*); once again, most islets showed no change in fluorescence, yet rare islets responded with acute loss of CpepSfGFP fluorescence (Fig. 8*F*), which was not seen in saline-infused controls. This surprising result strongly suggests that the insulin

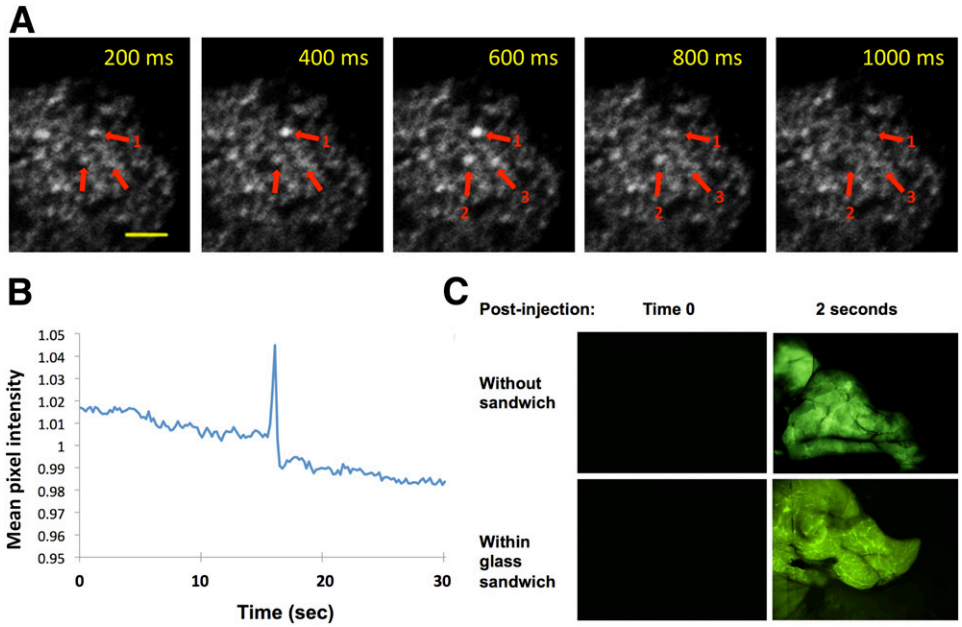

Figure 6— Pancreatic β-cell exocytosis, and blood flow to the live mouse pancreas under imaging conditions. *A*: From Supplementary Video 1, showing a series of 200-ms spinning disk confocal microscope fluorescence exposures of a β-cell stimulated with 60 mmol/L KCl (also seen with 25 mmol/L glucose); five sequential images (spanning 1 s) demonstrate the appearance of fluorescent insulin secretory granules and their disappearance after a "flash." Arrows highlight the locations before, during, and after the flash seen for three different granule fusion events. The flash reflects a neutral pH–elicited increase in CpepSfGFP fluorescence upon granule fusion followed by the rapid loss of signal as the released content disperses. *B*: Intensity trace documents the kinetics of fluorescence emission from a single granule exocytotic event. Specifically, the intensity of a region of interest was normalized to the mean intensity of that region of interest. The time indicated on the *x*-axis represents the time after the initiation of perfusion with KCl solution. Scale bar = 2.5 μm. *C*: The pancreata of live mice were externalized as described in the text, placed on a glass slide, and either sandwiched with an overlying glass coverslip or not. Animals on a warmed microscope stage were administered uranine (5 mg/mL) by jugular vein injection during live animal fluorescence imaging. The data are representative of five animals per group.

secretory response to acute stimulation in vivo includes a subset of islets that serve as "first responders" to the nutrient challenge.

DISCUSSION

Secretory granules are the essential storage pool for pancreatic secretory proteins, including insulin (20). In the steady state, normal humans maintain an intrapancreatic storage pool of insulin sufficient for ≥1 week of metabolic demand (21). In individuals with type 2 diabetes, pancreatic insulin stores decline, and this has been attributed to both β-cell death (22) and β-cell dedifferentiation (23). A major thrust of diabetes research in recent decades has focused on preventing these changes (24).

Despite potential differences between mouse and human pancreas, genetically engineered mice have been extremely valuable for proof-of-concept studies regarding the potential for visualization of pancreatic β-cells (25) and quantification of pancreatic β-cell mass (26). However, because increasing emphasis has been placed on pancreatic insulin content as a better measure of residual pancreatic function (27), our interest has shifted to develop a means to follow insulin mass rather than β-cell mass. Although it has not proved possible to directly label insulin for imaging in live animals, the next best thing is to follow costored C-peptide.

In the current study, we describe hPro-CpepSfGFP mice that were created with precisely this intent. This protein was already known to migrate successfully through the β-cell Golgi complex for processing and storage of human insulin (7). Using *Ins1* promoter–driven expression, the protein is expressed only in pancreatic islets (Fig. 1) and is limited exclusively to β-cells. The fluorescent proinsulin, like endogenous proinsulin, is efficiently processed to C-peptide (Fig. 2*A*) that is cosecreted with insulin (Fig. 4*C* and *D*). Pancreatic fluorescence in hPro-CpepSfGFP mice is not a perfect marker of processed insulin, as only ~85% of the epifluorescence is expected to report granule C-peptide (Fig. 2*B*), whereas the remaining 15% represents unprocessed (or incompletely processed) fluorescent proinsulin (7).

An hGH minigene was included to serve as an enhancer in the hPro-CpepSfGFP transgene construct, which has potential independent effects on pancreatic β-cell mass (28). Indeed, islets of hPro-CpepSfGFP mice did exhibit a threefold to fivefold increase in mRNA levels of tryptophan hydroxylase; however, these mRNA levels are ~100-fold to 2,000-fold lower than in islets of other

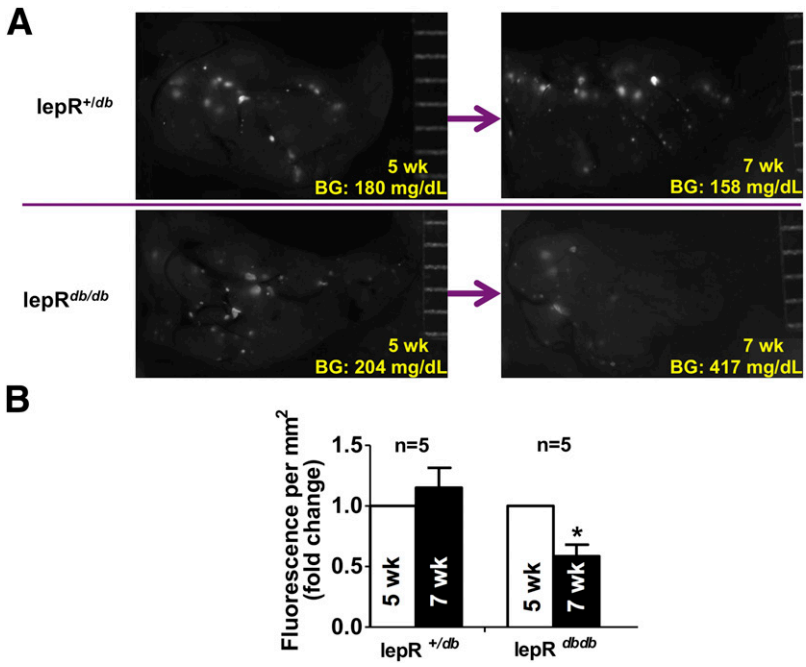

Figure 7—Live mouse pancreatic surface fluorescence imaging of islet CpepSfGFP. The pancreata of five transgenic hPro-CpepSfGFP lepR$^{db/db}$ mice and five hPro-CpepSfGFP lepR$^{db/+}$ control mice were examined by epifluorescence imaging (500-ms exposure) of the pancreatic surface of living animals, with images captured at 5 weeks of age and again at 7 weeks of age. A fluorescent ruler (right of each image) shows 1-mm spacing. *A*: Repeat analysis of the hPro-CpepSfGFP lepR$^{db/+}$ control mouse (top panels) shows a stable random blood glucose level (bottom right corner "BG") and no loss of surface fluorescence between 5 and 7 weeks. By contrast, repeat analysis of an hPro-CpepSfGFP lepR$^{db/db}$ mouse (bottom panels) shows the onset of frank diabetes (BG), and a decline of surface fluorescence between 5 and 7 weeks. *B*: Metamorph image analysis software was used to quantify the total integrated islet pixel intensity in the image divided by total pancreatic surface area in the image. Values are expressed as the mean ± SEM. *P < 0.05 at 7 weeks compared with 5 weeks in lepR$^{db/db}$ mice.

hGH minigene–containing transgenic models (28), and we have established that islets of hPro-CpepSfGFP do not exhibit increased β-cell proliferation or diminished cell death (data not shown). Further, in contrast with C57BL/6N mice, we used C57BL/6J mice that have functional deletion of the nicotinamide nucleotide transhydrogenase gene (29). However, recent studies (30) have shown that insulin secretion responses to an intragastric or intravenous glucose bolus are not different between C57BL/6J and C57BL/6N animals. Moreover, we are confident that the animals developed in this study, derived from two independent transgenic lineages, do not exhibit detectable metabolic differences from wild-type littermates, because both males and females exhibit normal fasting blood glucose levels, acute insulin responses, glucose tolerance (Fig. 3*A*–*F*), and body weight that are unaffected by aging. Further, these animals do not possess appreciably more pancreatic insulin when expressing the hPro-CpepSfGFP transgene because only 0.04% of total insulin plus proinsulin is composed of the human insulin component (Fig. 4*B*). Moreover, the transgene does not protect lepR*db*/^{db} animals from developing severe diabetes, which is accompanied by significant loss of pancreatic CpepSfGFP (Fig. 7).

The temporal release of fluorescent C-peptide appears indistinguishable from that of insulin using either static incubation of isolated islets (Fig. 5*A*) or dynamic release from individual islets measured using a sophisticated microfluidics analysis (Fig. 5*B*). Acute stimulation of individual β-cells yields unmistakable visual proof of granule exocytosis (Supplementary Video 1 and Fig. 6*A* and *B*), but this does not result in a discernible decrease of CpepSfGFP fluorescence from islets incubated in vitro. However, imaging of islet insulin content in vivo has never previously been examined, even as there is every reason to believe that in vivo fluorescence imaging of the pancreatic surface of hPro-CpepSfGFP mice provides a valid assessment of both pancreatic insulin content under basal conditions and insulin loss from islets upon acute or chronic stimulation. Our imaging modality does not impair blood delivery to the pancreas (Fig. 6*C*) but readily detects a decline in pancreatic insulin content during diabetes progression in *db*/*db* mice. In negative control animals given either intragastric (Fig. 8*A*) or intravenous saline (not shown), there is no acute loss of islet fluorescence (Fig. 8*B*). Remarkably, however, after acute intragastric or intravenous administration of glucose, the fluorescence intensity of most islets remains unchanged, but a

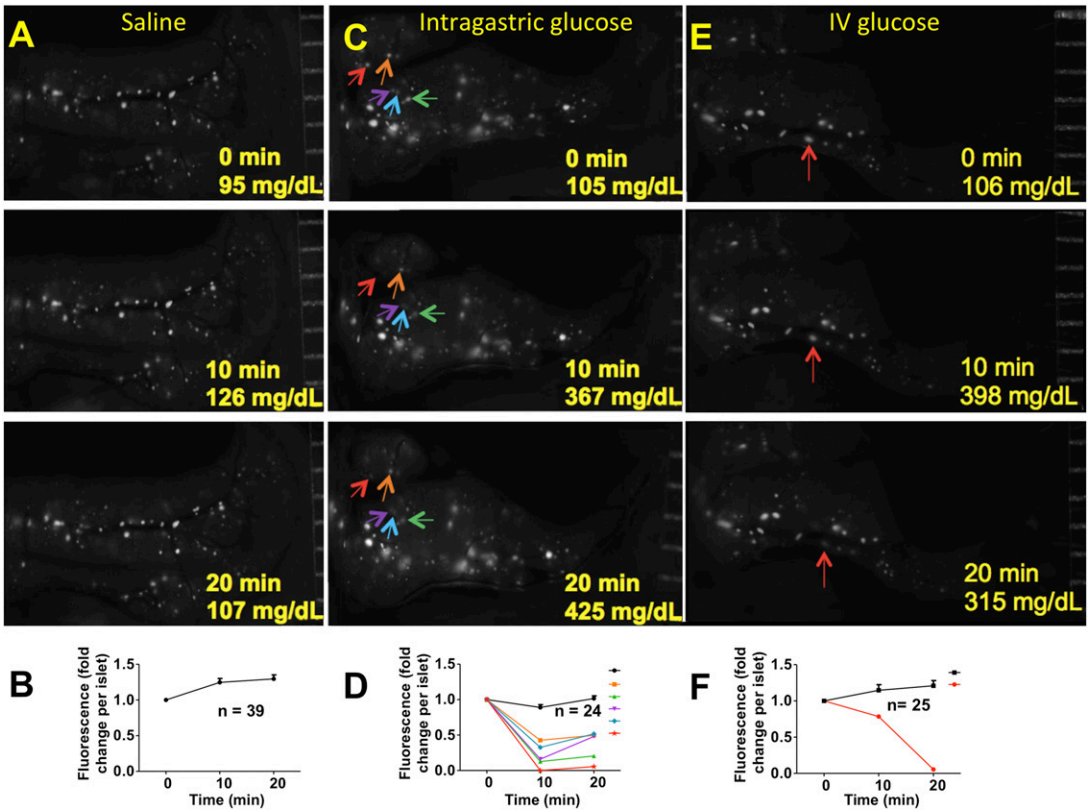

Figure 8—Pancreatic imaging after acute glucose administration to hPro-CpepSfGFP transgenic mice. Live hPro-CpepSfGFP transgenic mice were anesthetized for epifluorescence imaging of the pancreatic surface (500-ms exposure) as described in RESEARCH DESIGN AND METHODS. *A*: After initial image capture, saline was delivered to the stomach lumen at time 0, with subsequent images captured at 10 and 20 min (aligned vertically). Blood glucose from the tail vein was examined simultaneously (shown in the lower right corner of each image). A fluorescent ruler (right of each image) shows 1-mm spacing. Five animals were examined in each group with identical results—a representative set of images is shown—and five additional animals were imaged in this way, with identical results upon intravenous delivery of saline via jugular vein (data not shown). *B*: Fluorescence intensity of each surface islet from panel *A* at each time point was quantified using MetaMorph image analysis software, normalized to fluorescence intensity at time 0. Any islet that showed a ≥50% change in fluorescence intensity between time points was graphed individually instead of being included in the group analysis; no such islets were found in the control animals that were given saline. The data are plotted as the mean ± SEM. *C*: After initial image capture, glucose was delivered to the stomach lumen at time 0, with subsequent images aligned as in panel *A*. Individual islets that showed a ≥50% decrease in fluorescence intensity between time points were noted with colored arrows. Five animals were examined with similar results—a representative set of images is shown. *D*: Change in fluorescence intensity within individual islets imaged in panel *C*. The majority of islets showed no significant change in fluorescence intensity, and the signal from those islets was averaged with the *n* number shown ± SEM. Islets from the same pancreas that showed a ≥50% decrease of fluorescence intensity between time points were plotted individually, using colors matched to the arrows of panel *C*. *E*: After initial image capture, glucose was delivered via jugular vein at time 0, with subsequent images aligned as in panel *A*. Individual islets that showed a ≥50% decrease in fluorescence intensity between time points were noted with colored arrows. Five animals were examined with similar results—a representative set of images is shown. *F*: Data from panel *E* were quantified and plotted as in panel *D*.

subpopulation of imaged islets within the pancreas in vivo shows a ≥50% decrease in fluorescence (Fig. 8*C* and *D*), which is consistent with a major fraction of insulin released from this islet subset. Importantly, as noted in the introduction, Stefan et al. (14) also looked at acute secretory stimulation in vivo and reported dramatic but heterogeneous depletion of insulin stores from β-cells in the pancreatic tail—the same region that we have been imaging. However, their earlier work (31) used longer times of stimulation (and included sulfonylureas), whereas we limited our analysis to a 20-min postglucose challenge to exclude the powerful (but potentially confounding) stimulatory effects of glucose on the translation of new proinsulin. Our data thus suggest that upon an acute increase in blood glucose level, islet first responders contribute disproportionately to initial insulin secretory response in vivo.

We must reiterate that all our intravital imaging experiments were performed under anesthesia that can affect blood pressure or may alter central nervous system neural outputs to pancreatic islets—and might also be affected by tissue oxygenation and breathing (32). Further, we have yet to discern a spatial pattern to predict first responder islets that may be preferentially activated via the nervous system or by favorable nutrient delivery originating from splenic and mesenteric arteries. Regardless, it is tempting to speculate that, based on these

findings, "pancreatic exhaustion" might be initiated as a patchy defect, caused by initial secretory overactivity and insulin depletion in first-responder islets.

Acknowledgments. The authors thank Bill and Dee Brehm for advancing diabetes research at the University of Michigan. The authors also thank Jiane Feng and Nathan Qi (University of Michigan Animal Phenotyping Core) for assistance with jugular vein injection and Nikita Jaber (University of Michigan, Division of Metabolism, Endocrinology & Diabetes) for technical assistance.

Funding. This work was funded primarily by National Institutes of Health (NIH) grant R01-DK-48280 (to P.A.) and also by grants R37-DK-046960 (to R.K.) and R01-DK-091296 (to D.C.). Financial assistance was also received from the NIH-funded Diabetes Research Center grant P60-DK-20572 and Nutrition Obesity Research Centers grant P30-DK-089503 for support of the University of Michigan Transgenic Core, Animal Phenotyping Core, Administrative and Molecular Biology Core, and the Morphology and Image Analysis core.

Duality of Interest. No potential conflicts of interest relevant to this article were reported.

Author Contributions. S.Z. researched the data, contributed to the discussion, wrote the article, and reviewed and edited the article. D.L., S.L., C.I., R.K., and D.C. researched the data, contributed to the discussion, and reviewed and edited the article. L.H. researched the data, and reviewed and edited the article. A.A. researched the data and contributed to the discussion. P.A. contributed to the discussion, wrote the article, and reviewed and edited the article. P.A. is the guarantor of this work and, as such, had full access to all the data in the study and takes responsibility for the integrity of the data and the accuracy of the data analysis.

References

1. Alejandro EU, Gregg B, Blandino-Rosano M, Cras-Méneur C, Bernal-Mizrachi E. Natural history of β-cell adaptation and failure in type 2 diabetes. Mol Aspects Med 2015;42:19–41

2. Meier JJ, Bonadonna RC. Role of reduced β-cell mass versus impaired β-cell function in the pathogenesis of type 2 diabetes. Diabetes Care 2013; 36(Suppl. 2):S113–S119

3. DeFronzo RA, Bonadonna RC, Ferrannini E. Pathogenesis of NIDDM. A balanced overview. Diabetes Care 1992;15:318–368

4. Alarcon C, Boland BB, Uchizono Y, et al. Pancreatic β-cell adaptive plasticity in obesity increases insulin production but adversely affects secretory function. Diabetes. 25 August 2015 [Epub ahead of print]. DOI: 10.2337/db15-0792

5. Masini M, Marselli L, Bugliani M, et al. Ultrastructural morphometric analysis of insulin secretory granules in human type 2 diabetes. Acta Diabetol 2012;49(Suppl. 1):S247–S252

6. Hodish I, Liu M, Rajpal G, et al. Misfolded proinsulin affects bystander proinsulin in neonatal diabetes. J Biol Chem 2010;285:685–694

7. Haataja L, Snapp E, Wright J, et al. Proinsulin intermolecular interactions during secretory trafficking in pancreatic β cells. J Biol Chem 2013;288:1896–1906

8. Sizonenko S, Irminger J-C, Buhler L, Deng S, Morel P, Halban PA. Kinetics of proinsulin conversion in human islets. Diabetes 1993;42:933–936

9. Poitout V, Stein R, Rhodes CJ. Insulin gene expression and biosynthesis. In *International Textbook of Diabetes Mellitus*. 4th ed. DeFronzo RA, Ferrannini E, Zimmet P, Alberti KGMM, eds. Hoboken, NJ, John Wiley & Sons, 2004, p. 97–123

10. Barg S, Eliasson L, Renström E, Rorsman P. A subset of 50 secretory granules in close contact with L-type Ca2+ channels accounts for first-phase insulin secretion in mouse β-cells. Diabetes 2002;51(Suppl. 1):S74–S82

11. Hou JC, Min L, Pessin JE. Insulin granule biogenesis, trafficking and exocytosis. Vitam Horm 2009;80:473–506

12. Rorsman P, Eliasson L, Renström E, Gromada J, Barg S, Göpel S. The cell physiology of biphasic insulin secretion. News Physiol Sci 2000;15:72–77

13. Chen M, Porte D Jr. The effect of rate and dose of glucose infusion on the acute insulin response in man. J Clin Endocrinol Metab 1976;42:1168–1175

14. Stefan Y, Meda P, Neufeld M, Orci L. Stimulation of insulin secretion reveals heterogeneity of pancreatic B cells in vivo. J Clin Invest 1987;80:175–183

15. Pédelacq JD, Cabantous S, Tran T, Terwilliger TC, Waldo GS. Engineering and characterization of a superfolder green fluorescent protein. Nat Biotechnol 2006;24:79–88

16. Dishinger JF, Reid KR, Kennedy RT. Quantitative monitoring of insulin secretion from single islets of Langerhans in parallel on a microfluidic chip. Anal Chem 2009;81:3119–3127

17. Michael DJ, Ritzel RA, Haataja L, Chow RH. Pancreatic β-cells secrete insulin in fast- and slow-release forms. Diabetes 2006;55:600–607

18. Perrais D, Kleppe IC, Taraska JW, Almers W. Recapture after exocytosis causes differential retention of protein in granules of bovine chromaffin cells. J Physiol 2004;560:413–428

19. Tozzo E, Ponticiello R, Swartz J, et al. The dual peroxisome proliferator-activated receptor alpha/gamma activator muraglitazar prevents the natural progression of diabetes in db/db mice. J Pharmacol Exp Ther 2007;321:107–115

20. Arvan P, Castle D. Sorting and storage during secretory granule biogenesis: looking backward and looking forward. Biochem J 1998;332:593–610

21. Rahier J, Guiot Y, Goebbels RM, Sempoux C, Henquin JC. Pancreatic beta-cell mass in European subjects with type 2 diabetes. Diabetes Obes Metab 2008; 10(Suppl. 4):32–42

22. Montane J, Cadavez L, Novials A. Stress and the inflammatory process: a major cause of pancreatic cell death in type 2 diabetes. Diabetes Metab Syndr Obes 2014;7:25–34

23. Talchai C, Xuan S, Lin HV, Sussel L, Accili D. Pancreatic β cell dedifferentiation as a mechanism of diabetic β cell failure. Cell 2012;150:1223–1234

24. Weir GC, Bonner-Weir S. Islet β cell mass in diabetes and how it relates to function, birth, and death. Ann N Y Acad Sci 2013;1281:92–105

25. Hara M, Dizon RF, Glick BS, et al. Imaging pancreatic beta-cells in the intact pancreas. Am J Physiol Endocrinol Metab 2006;290:E1041–E1047

26. Kilimnik G, Kim A, Jo J, Miller K, Hara M. Quantification of pancreatic islet distribution in situ in mice. Am J Physiol Endocrinol Metab 2009;297:E1331–E1338

27. Ferrannini E. The stunned beta cell: a brief history. Cell Metab 2010;11: 349–352

28. Brouwers B, de Faudeur G, Osipovich AB, et al. Impaired islet function in commonly used transgenic mouse lines due to human growth hormone minigene expression. Cell Metab 2014;20:979–990

29. Freeman HC, Hugill A, Dear NT, Ashcroft FM, Cox RD. Deletion of nicotinamide nucleotide transhydrogenase: a new quantitive trait locus accounting for glucose intolerance in C57BL/6J mice. Diabetes 2006;55:2153–2156

30. Wong N, Blair AR, Morahan G, Andrikopoulos S. The deletion variant of nicotinamide nucleotide transhydrogenase (Nnt) does not affect insulin secretion or glucose tolerance. Endocrinology 2010;151:96–102

31. Alarcón C, Lincoln B, Rhodes CJ. The biosynthesis of the subtilisin-related proprotein convertase PC3, but no that of the PC2 convertase, is regulated by glucose in parallel to proinsulin biosynthesis in rat pancreatic islets. J Biol Chem 1993;268:4276–4280

32. Cao L, Kobayakawa S, Yoshiki A, Abe K. High resolution intravital imaging of subcellular structures of mouse abdominal organs using a microstage device. PLoS One 2012;7:e33876